

Deposition conditions and electrical properties of relaxor ferroelectric $\text{Pb}(\text{Fe}_{1/2}\text{Nb}_{1/2})\text{O}_3$ thin films prepared by pulsed laser deposition

Li Yan, Jiefang Li, and D. Viehland

Citation: *Journal of Applied Physics* **101**, 104107 (2007); doi: 10.1063/1.2724592

View online: <http://dx.doi.org/10.1063/1.2724592>

View Table of Contents: <http://scitation.aip.org/content/aip/journal/jap/101/10?ver=pdfcov>

Published by the [AIP Publishing](#)

Articles you may be interested in

Enhanced ferroelectric and dielectric properties of (111)-oriented highly cation-ordered $\text{PbSc}_{0.5}\text{Ta}_{0.5}\text{O}_3$ thin films

J. Appl. Phys. **114**, 224109 (2013); 10.1063/1.4846817

Dielectric properties of lead lanthanum zirconate stannate titanate antiferroelectric thin films prepared by pulsed laser deposition

J. Appl. Phys. **95**, 6341 (2004); 10.1063/1.1715136

Dielectric and electromechanical properties of $\text{Pb}(\text{Mg}_{1/3}, \text{Nb}_{2/3})\text{O}_3 - \text{PbTiO}_3$ thin films grown by pulsed laser deposition

J. Appl. Phys. **93**, 9924 (2003); 10.1063/1.1574181

Dielectric properties of pulsed laser deposited films of $\text{PbMg}_{1/3}\text{Nb}_{2/3} - \text{PbTiO}_3$ and $\text{PbSc}_{1/2}\text{Nb}_{1/2}\text{O}_3 - \text{PbTiO}_3$ relaxor ferroelectrics

J. Appl. Phys. **86**, 5179 (1999); 10.1063/1.371497

Phase development and electrical property analysis of pulsed laser deposited $\text{Pb}(\text{Mg}_{1/3}\text{Nb}_{2/3})\text{O}_3 - \text{PbTiO}_3$ (70/30) epitaxial thin films

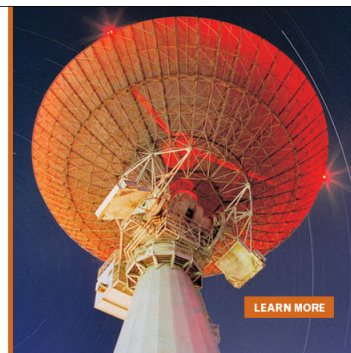
J. Appl. Phys. **84**, 5147 (1998); 10.1063/1.368809

MIT LINCOLN
LABORATORY
CAREERS

Discover the satisfaction of
innovation and service
to the nation

- Space Control
- Air & Missile Defense
- Communications Systems & Cyber Security
- Intelligence, Surveillance and Reconnaissance Systems
- Advanced Electronics
- Tactical Systems
- Homeland Protection
- Air Traffic Control

 **LINCOLN LABORATORY**
MASSACHUSETTS INSTITUTE OF TECHNOLOGY



Deposition conditions and electrical properties of relaxor ferroelectric $\text{Pb}(\text{Fe}_{1/2}\text{Nb}_{1/2})\text{O}_3$ thin films prepared by pulsed laser deposition

Li Yan,^{a)} Jiefang Li, and D. Viehland

Department of Materials Science and Engineering, Virginia Tech, Blacksburg, Virginia 24061

(Received 5 October 2006; accepted 6 March 2007; published online 24 May 2007)

Epitaxial lead iron niobate thin films with thicknesses of $50 \text{ nm} < t < 500 \text{ nm}$ have been deposited by pulsed laser deposition. We have identified the deposition conditions that result in insulating layers. These critical conditions are essential to (i) prevent semiconducting resistivity characteristics, (ii) achieve higher induced polarizations of $70 \mu\text{C}/\text{cm}^2$ under $E=190 \text{ kV}/\text{mm}$, and (iii) obtain remanent polarizations of $17.7 \mu\text{C}/\text{cm}^2$, coercive fields of $9.5 \text{ kV}/\text{mm}$, and dielectric constants of ~ 1200 at room temperature. © 2007 American Institute of Physics.

[DOI: [10.1063/1.2724592](https://doi.org/10.1063/1.2724592)]

I. INTRODUCTION

Lead iron niobate, $\text{Pb}(\text{Fe}_{1/2}\text{Nb}_{1/2})\text{O}_3$ or PFN, is a relaxor ferroelectric that was originally reported by Smolenkii *et al.* in 1964.¹ It has a paraelectric \rightarrow ferroelectric transformation near a Curie Temperature of $T_C=385 \text{ K}$.^{1,2} The room temperature lattice structure of PFN single crystals is rhombohedral with lattice parameters of $a_r=4.0123 \text{ \AA}$ and $\alpha_r=89.89^\circ$.^{1,3-5} The maximum polarization has been reported to be only $\sim 10 \mu\text{C}/\text{cm}^2$;⁶ the polarization electric field (P - E) response is “nonsquare” yet hysteretic at room temperature; the dielectric breakdown field is low; and the weak-field dielectric loss factor is quite high. These limited dielectric and ferroelectric properties of bulk crystals and ceramics are believed to reflect inferior dielectric insulation.

Many investigations on $\text{Pb}(\text{Mg}_{1/3}\text{Nb}_{2/3})\text{O}_{3-x}$ at. % PbTiO_3 (PMN- x PT) and $\text{Pb}(\text{Zn}_{1/3}\text{Nb}_{2/3})\text{O}_{3-x}$ at. % PbTiO_3 (PZN- x PT) relaxor thin layers have been performed. High-quality epitaxial single crystal layers have been reported.⁷⁻¹² The said studies have revealed that the dielectric constant maximum of bulk specimens ($K_{\text{max}} \approx 30\,000$) are notably reduced in thin-film form ($K_{\text{max}} \approx 3000$).¹³⁻¹⁵ Compared with PMN-PT, only a few papers have been published on PFN thin layers. Nonepitaxial films with superior properties have been reported by Sedlar and Sayer¹⁶ using a sol-gel method. After rapid thermal processing at 923 K – 973 K , the permittivity of PFN films was reported to be increased to $K=1000$, and its maximum polarization increased to $P=24 \mu\text{C}/\text{cm}^2$, which are equal (K) or superior (P) to those reported for bulk crystals and ceramics. Nonepitaxial PFN films have also been deposited by pulsed laser deposition.^{17,18} However, unfortunately, the resultant properties were found to be inferior to bulk crystals and ceramics, for example, dielectric constants of 200 – 400 at room temperature. In consideration that sol-gel films have equivalent or superior properties to crystals/ceramics, it is reasonable to anticipate that significant improvements in the properties of epitaxial PFN films might be achieved by studying the film deposition conditions.

Here, we present the results of an investigation that identifies the influence of various deposition conditions—temperature, oxygen partial pressure, laser frequency, film thickness—on PFN thin films prepared by pulsed laser deposition (PLD). We have found that these conditions are very critical to obtaining films with superior properties: only in a narrow deposition window can highly resistive ($10^9 \Omega \text{ cm}$) PFN films be achieved, which is at a critical insulation threshold required for dielectric applications. For these insulating films, we report (i) induced polarizations of $70 \mu\text{C}/\text{cm}^2$ under $E=190 \text{ kV}/\text{mm}$ and (ii) dielectric constants of ~ 1200 at room temperature.

II. EXPERIMENTAL PROCEDURE

In order to ensure the stoichiometric ratio of different ions, targets of PFN were prepared using a one-step solid-state reaction method. Powders of PbO (99.9%), Fe_2O_3 (99.945%) and Nb_2O_5 (99.9%) were batched in stoichiometric ratio with an excess of 5% PbO ; ball milled for 12 h in isopropanol solution; calcined at 1123 K for 3 h; and subsequently remilled, sieved, and powder pressed into a tablet under 30 kpsi. The tablets were sintered for 3 h by controlled atmosphere sintering to reduce Pb loss using $\text{PbO}+\text{PbO}_2+\text{ZrO}_2$ powder. Epitaxial thin films of PFN were then deposited by PLD using these targets. Deposition was done on (001)-oriented SrTiO_3 substrates, and films with thicknesses of $50 < t < 500 \text{ nm}$ were grown. The energy density of the KrF laser (Lambda 305i) was $1.6 \text{ J}/\text{cm}^2$ at a wavelength of 248 nm . The distance between the target and substrate was 6 cm . The growth rate of the PFN thin films was, for example, $10 \text{ nm}/\text{min}$ at a deposition temperature of 903 K . A 50 nm SrRuO_3 layer was used as a bottom electrode, which was deposited by PLD at 923 K using a growth rate of $0.7 \text{ nm}/\text{min}$. A $38 \times 38 \mu\text{m}^2$ top gold electrode was then deposited by sputtering. Films were grown at various deposition temperatures, oxygen partial pressures, laser frequencies, and thicknesses.

The structural and ferroelectric properties of the thin films were measured. X-ray diffraction (XRD) studies were performed using a Philips X’pert high-resolution system equipped with a two-bounce hybrid monochromator and an

^{a)}Electronic mail: lyan@vt.edu

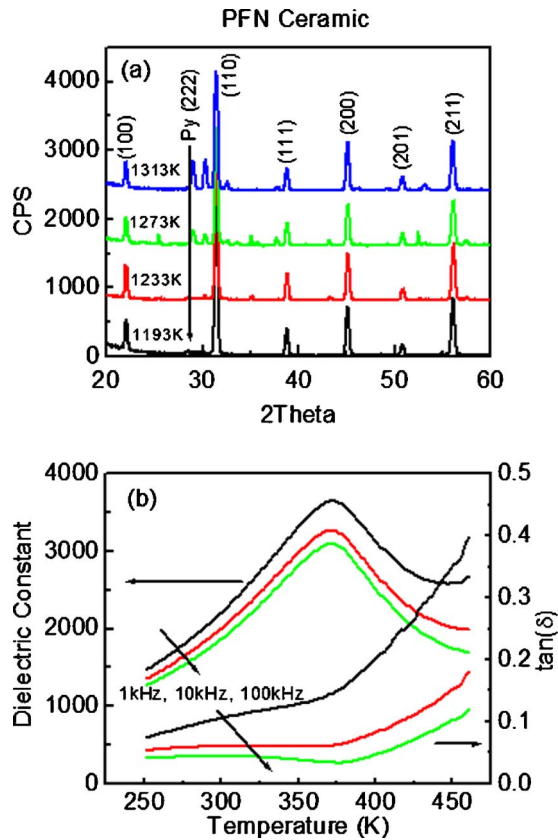


FIG. 1. XRD and dielectric constant results of PFN ceramics. (a) Line scan over wide angles of PFN ceramics sintered at different temperatures and (b) dielectric constant and loss as a function of temperature for various frequencies.

open three-circle Eulerian cradle. The analyzer was a Ge (220) cut crystal which had a θ resolution of 0.0068° . The x-ray unit was operated at 45 kV and 40 mA with a wavelength of 1.5406 \AA ($\text{Cu } K\alpha$). A Radiant Technology precision workstation was used to measure the resistivity and polarization of the PFN thin films and a HP4284 LCR meter equipped with a MMR thermal stage was used to measure the dielectric constant as a function of temperature.

III. RESULTS AND DISCUSSION

A. Fabrication and testing of PFN targets

Targets of PFN were sintered at different temperatures ranging from 1193 to 1313 K. XRD line scans of these targets sintered at different temperatures are given in Fig. 1(a). The target sintered at 1193 K was almost phase-pure perovskite, having only 1.6% volume fraction of a secondary pyrochlore phase. The phase purity was calculated by

$$\% \text{ pyrochlore} = \frac{I_{\text{pyro}(222)}}{I_{\text{pyro}(222)} + I_{\text{perov}(110)}} \times 100 \%,$$

where $I_{\text{pyro}(222)}$ is the intensity of the (222) pyrochlore peak and $I_{\text{perov}(110)}$ that of the (110) perovskite peak. However, with increasing sintering temperature, the %pyrochlore increased markedly and with other undetermined impurity peaks appearing. Also, with increasing sintering temperature, the density of the targets decreased, which demonstrates el-

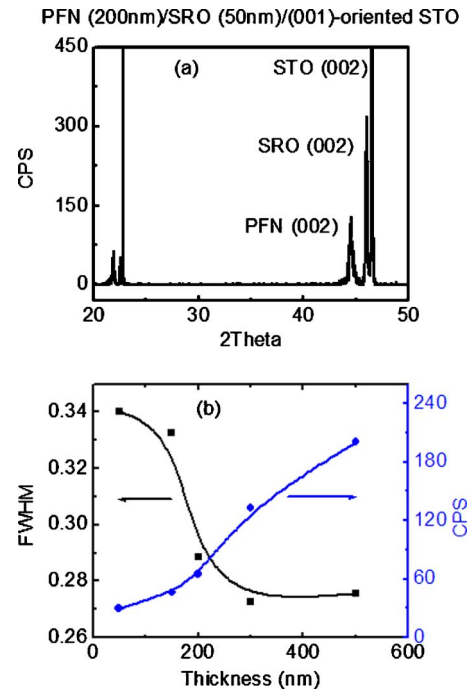


FIG. 2. XRD results of PFN thin films. (a) Line scan over wide angles, demonstrating phase purity and good epitaxy and (b) full width at half maximum (FWHM) and intensity of PFN (002) peaks (2θ) as a function of thickness.

emental loss on firing (presumably PbO). In order to maintain proper stoichiometry of the PFN target, we chose the one sintered at 1193 K to be used for film deposition.

The dielectric constant of this PFN target (sintered at 1193 K) is shown in Fig. 1(b). At room temperature, the values of the dielectric constant and loss factor are about $K = 2000$ and $\tan \delta = 0.05$ at $V_{\text{ac}} = 1 \text{ V}$, respectively. The value of the dielectric constant and loss factor were both decreased with increasing measurement frequency, which is unlike that typical of a relaxor ferroelectric, where $\tan \delta$ increases with increasing frequency. The temperature dependent dielectric response revealed that the Curie temperature, determined by the temperature of the dielectric maximum (T_{max}), was $T_C \approx 370 \text{ K}$. A frequency dispersion of T_{max} was not distinct in the figure, as conventional expected of a relaxor ferroelectric.

B. Confirmation of film epitaxy by XRD

The PFN thin films deposited on (001) $\text{SrRuO}_3/\text{SrTiO}_3$ (SRO/STO) were all found to be epitaxial phase-pure perovskites, as illustrated in Fig. 2(a). Unlike for the PFN ceramic targets, we found no pyrochlore peaks by XRD in the films. The (002) peaks of PFN, SRO, and STO were at 44.42° , 45.99° , and 46.49° , respectively. With increasing film thickness, the full width half maximum (FWHM) decreased dramatically, as shown in Fig. 2(b), but for $t > 200 \text{ nm}$, it was nearly unchanged ($\text{FWHM} = 0.27^\circ$) with further increase of thickness. In addition, with increasing film thickness, the intensity of its (002) reflection can be seen to increase quasi-linearly, simply because the thicker the film, the more planes from which to reflect. The structure of the (001) PFN films was recently discussed in another paper.¹⁹

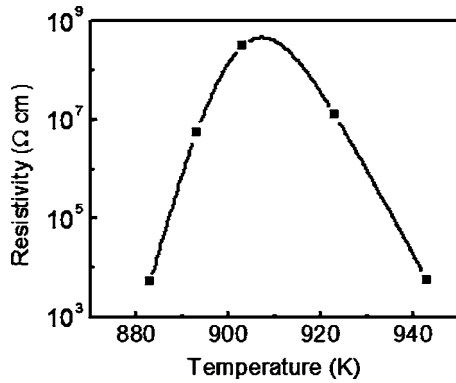


FIG. 3. Resistivity of PFN thin film as a function of growth temperature.

C. Identification of optimum deposition conditions: ρ and P - E

For most perovskites, the deposition temperature window over which phase-pure films form is quite broad. In the case of PFN, phase pure perovskite films were formed from 883 to 943 K. However, unfortunately, we found that the corresponding temperature window for achieving highly resistive films was quite narrow, as shown in Fig. 3. For a deposition temperature of 903 K, the resistivity of PFN reached values of up to $\rho > 5 \times 10^8 \Omega \text{ cm}$, but decreased by nearly five orders of magnitude to $\rho = 5 \times 10^3 \Omega \text{ cm}$, if the deposition temperature was changed by only 20 K. Clearly, the temperature window over which insulating PFN films can be deposited is unusually narrow, consistent with difficulties in precisely tuning to an optimum stoichiometry.

We then determined the effects of ambient oxygen pressure (P_{O_2}) from 15 mTorr to 150 mTorr and of laser frequency changes (ν) by 5–40 Hz. The polarization curves for four PFN thin layers deposited under different P_{O_2} and ν conditions are given in Fig. 4. From these P - E curves, we can identify that the best deposition condition was for ν

$= 30 \text{ Hz}$ and $P_{\text{O}_2} = 20 \text{ mTorr}$. Only under these particular conditions was a slim P - E loop obtained: clearly, the deposition condition windows for insulating PFN layers capable of withstanding high voltages are very narrow. The gap at the bottom of the P - E curve at $E=0$ reflects the presence of a Schottky barrier ($\Delta\phi$) at the interface between the metal electrodes and PFN layer. If the resistivity of the film is $\rho \geq 10^9$, this gap is quite small, as can be seen in part (b) of the figure. Furthermore, the shape of the P - E response was found to be strongly dependent on ρ : if ρ is small, the P - E curve was more rounded and hysteretic, rather than sharp and slim. These results demonstrate the extreme sensitivity of the high voltage characteristics of PFN films on oxygen stoichiometry, in addition to that on temperature: there is very limited flexibility in deposition conditions that allow achievement of high voltage insulation.

We next determined the effect of annealing time and cooling rate (data not shown). It was found that a 10 min anneal was sufficient to achieve insulating films (for films deposited under otherwise optimum conditions), and that longer annealing times did not improve either ρ or the ferroelectric polarization characteristics. Furthermore, a cooling rate of 5 K/min was found sufficiently slow to achieve these desired electrical properties. Finally, we mention that the energy of the laser notably affects film properties. If the energy is too low, the ratio of metal ions in the plasma is not the same as that of the target. This is because PbO easily evaporates from the target, whereas Nb does not. Alternatively, if the energy of the laser is too high, the surface of the film becomes rough and does not crystallize well. Our experience identified that laser energies of 1.6 mJ/cm^2 were best suited for PFN deposition.

D. Effect of film thickness on ρ and P

The effect of film thickness was then investigated for $50 \text{ nm} < t < 500 \text{ nm}$. In Fig. 5(a), the dependence of ρ on t is shown. The resistivity was nearly independent of thickness for $t > 200 \text{ nm}$, with $\rho \approx 10^9 \Omega \text{ cm}$. However, it decreased in a near linear manner with decreasing thickness below this critical value, reaching $\rho \approx 10^6 \Omega \text{ cm}$ for $t = 50 \text{ nm}$. In the experiment, PFN thin films over the thickness range from 50 to 500 nm were studied.

Accordingly, only thicker PFN films could sustain sufficiently high electric fields that were capable of inducing significant polarization changes. Figure 5(b) shows the corresponding dependence of the maximum induced polarization (P_{max}) on film thickness, which can also be seen to increase with increasing t . Inspection of this figure will reveal for thicker films that $P_{\text{max}} \leq 70 \mu\text{C/cm}^2$ could be induced, whereas, extrapolation of P_{max} to $t=0$ yielded extraneous values of $\leq 10 \mu\text{C/cm}^2$ consistent with previously reported values for bulk crystals/ceramics. This finding of higher induced polarizations in films is due to the simple fact that very high electric fields could be applied to the films before dielectric breakdown occurred and do not (as far as we can tell) result from an intrinsic polarization change with t . This is further illustrated in Fig. 6, which shows that P_{max} increases nearly linearly with increasing electric field for E

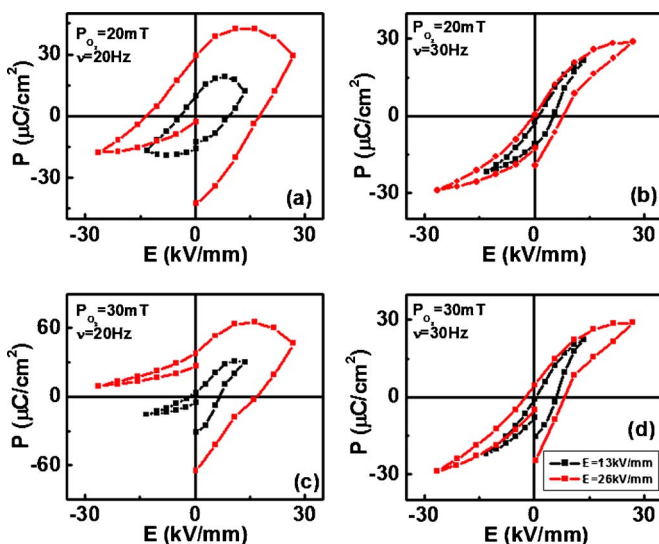


FIG. 4. P - E curves of PFN thin film as a function of oxygen pressure and laser frequency. (a) Oxygen pressure is 20 mTorr and laser frequency is 20 Hz; (b) oxygen pressure is 20 mTorr and laser frequency is 30 Hz; (c) oxygen pressure is 30 mTorr and laser frequency is 20 Hz; and (d) oxygen pressure is 30 mTorr and laser frequency is 30 Hz.

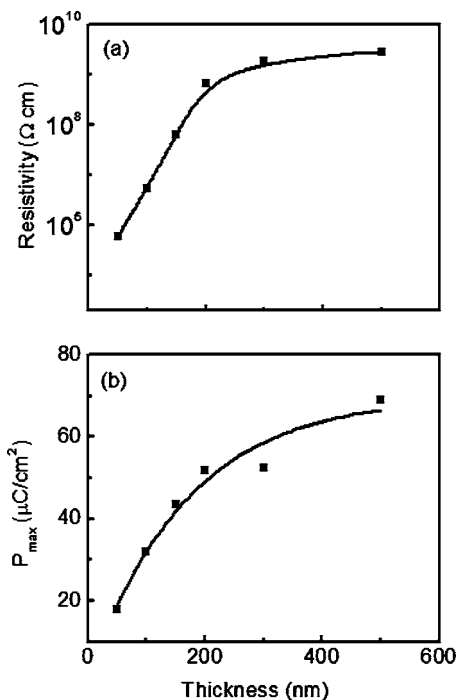


FIG. 5. Resistivity and maximum polarization of PFN thin films. (a) Resistivity of PFN thin films as a function of thickness and (b) maximum polarization of PFN thin films as a function of thickness from 50 to 500 nm.

> 50 kV/mm until, that is, dielectric breakdown occurs. Basically, the polarization does not saturate! Field levels as high as $E=190 \text{ kV/mm}$ could be sustained on films of thickness $t \approx 500 \text{ nm}$. It is also interesting to note in spite of this large P_{max} that the remanent polarization was only $P_r = 17 \mu\text{C}/\text{cm}^2$, with a small coercive field of $E_c=9 \text{ kV/mm}$.

Clearly, the ferroelectric polarization characteristics of PFN layers are unique offering (i) low remnant polarizations

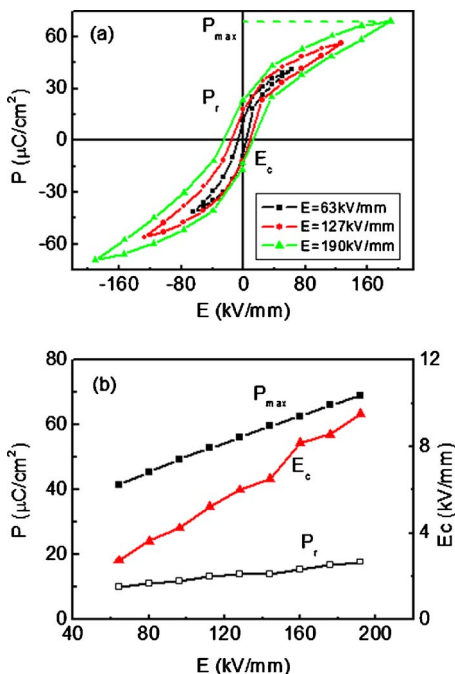


FIG. 6. Polarization of PFN thin films. (a) P - E curves of PFN thin film for different maximum electric fields and (b) P_{max} , E_c , and P_r of PFN thin films as a function of electric field.

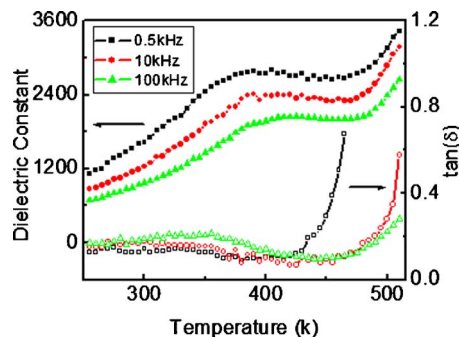


FIG. 7. Dielectric constant and loss of PFN thin film as a function of temperature for various frequencies.

(P_r), (ii) low coercive fields (E_c), (iii) large induced polarizations, in particular, relative to P_r , and (iv) slim P - E loops with low hysteretic losses, typical of a relaxor ferroelectric. These findings are in stark comparisons to the lossy P - E loops of bulk PFN ceramics/crystals which have low induced polarizations. Interestingly, the thinner films had resistivities and P - E responses similar to that of bulk crystals/ceramics than thicker films, $\rho \approx 10^5 \Omega \text{ cm}$ and $P_{\text{max}} \approx 10 \mu\text{C}/\text{cm}^2$. This fact underscores the unusual nature of the narrow deposition windows required to make sufficiently insulating PFN films, suggesting an important role in achieving a specific cation stoichiometry that limits spatial dimensions over which valence band hopping can occur.

E. Phase transformation characteristics: Temperature dependence of K

Figure 7 shows the temperature dependent complex dielectric constant for various measurement frequencies at $V_{\text{ac}}=0.1 \text{ V}$. The data reveal a frequency dispersion of the dielectric constant, where K decreases with increasing frequency, with T_{max} shifting to higher temperatures. Such dielectric dispersion is typical of a relaxor ferroelectric. The Curie temperature range was in the vicinity of 375 to 400 K, consistent with that of bulk ceramics [see Fig. 1(b)]. These findings demonstrate that epitaxial constraint does not alter the phase transformational characteristics.

It is also relevant to note that the dielectric loss factor ($\tan \delta$) increased with increasing frequency. This is unlike that for bulk PFN ceramics [see Fig. 1(b)], which decreased with increasing frequency, due to relaxing out of the space charge polarization mechanism. Rather, again, this component of the dielectric response is similar to that found in relaxor ferroelectrics. At higher temperatures, greater than the Curie range, clear evidence of space charge polarization contributions to the loss was evident. The onset of conduction contributions at $T > 400 \text{ K}$ correlate to corresponding increases in the real component of the response towards a secondary maximum. These findings furthermore underscore the fact that we have suppressed conduction in our PFN films by careful tuning of the deposition window.

IV. CONCLUSION

To achieve resistivities of $>10^9 \Omega \text{ cm}$, a minimum critical criterion for dielectric insulators, the deposition condi-

tions of PFN need to be restricted to a very narrow deposition window: 903 K deposition temperature, 20 mTorr oxygen pressure, and 30 Hz laser frequency (using the chamber we built at Virginia Tech). Changes of only 10 K in temperature, 10 mTorr in oxygen pressure, or 10 Hz in laser frequency result in a dramatic decrease in resistivity. Because of the higher resistivity in films prepared within this narrow deposition window, we can (i) sustain higher applied electric fields of up to $E < 190$ kV/mm; (ii) achieve induced polarizations of up to $70 \mu\text{C}/\text{cm}^2$, which are three times (seven times) higher than prior reported values for PFN films (crystals); and (iii) offer dielectric constants of up to $K = 1200$ at room temperature.

ACKNOWLEDGMENTS

We would like to gratefully acknowledge financial support from the U.S. Department of Energy under Contract No. DE.-AC02-98CH10886 and the Office of the Air-Force Office of Scientific Research under FA 9550-06-1-0410.

- ¹G. A. Smolenskii, A. Agranovskaya, S. N. Popov, and V. A. Isupov, *Sov. Phys. Tech. Phys.* **28**, 2152 (1958).
²G. L. Platonov, L. A. Drobyshev, Y. Y. Tomashpolskii, and Y. N. Venevsev, *Sov. Phys. Crystallogr.* **14**, 692 (1970).
³V. A. Vokov, I. E. Mylnikova, and G. A. Smolenskii, *Sov. Phys. JETP* **15**,

447 (1962).

- ⁴Y. Yang, J. M. Liu, H. B. Huang, W. Q. Zou, P. Bao, and Z. G. Liu, *Phys. Rev. B* **70**, 132101 (2004).
⁵Y. Yang, S. T. Zhang, H. B. Huang, Y. F. Chen, Z. G. Liu, and J. M. Liu, *Mater. Lett.* **59**, 1767 (2005).
⁶O. Raymond, R. Font, N. Suárez-Almodovar, J. Portelles, and J. M. Siqueiros, *J. Appl. Phys.* **97**, 084107 (2005).
⁷J. P. Maria, W. Hackenberger, and S. Trolier-McKinstry, *J. Appl. Phys.* **84**, 5147 (1998).
⁸G. R. Bai *et al.*, *Appl. Phys. Lett.* **76**, 3106 (2000).
⁹Y. L. Lu, J. J. Zheng, M. C. Golomb, F. L. Wang, H. A. Jiang, and J. Zhao, *Appl. Phys. Lett.* **74**, 3766 (1999).
¹⁰J. E. Spanier, M. Levy, I. P. Herman, R. M. Osgood, and A. S. Bhala, *Appl. Phys. Lett.* **79**, 1510 (2001).
¹¹K. Wasa *et al.*, *Appl. Phys. Lett.* **88**, 122903 (2006).
¹²S. Yokoyama, S. Okamoto, K. Saito, H. Uchida, S. Koda, and H. Funakubo, *Jpn. J. Appl. Phys., Part 2* **44**, L1452 (2005).
¹³V. Nagarajan, C. S. Ganpule, B. Nagaraj, S. Aggarwal, S. P. Alpay, A. L. Roytburd, E. D. Williams, and R. Ramesh, *Appl. Phys. Lett.* **75**, 4183 (1999).
¹⁴N. J. Donnelly, G. Catalan, C. Morros, R. M. Bowman, and J. M. Gregg, *J. Appl. Phys.* **93**, 9924 (2003).
¹⁵R. Ranjith, A. Sarkar, A. Laha, S. B. Krupanidhi, A. K. Balamurugan, S. Rajagoplan, and A. K. Tyagi, *J. Appl. Phys.* **98**, 014105 (2005).
¹⁶M. Sedlar and M. Sayer, *J. Appl. Phys.* **80**, 372 (1996).
¹⁷X. S. Gao, X. Y. Chen, J. Yin, J. Wu, Z. G. Liu, and M. Wang, *J. Mater. Sci.* **35**, 5421 (2000).
¹⁸X. R. Wang, S. S. Fan, Q. Q. Li, B. L. Gu, and X. W. Zhang, *Jpn. J. Appl. Phys., Part 2* **35**, L1002 (1996).
¹⁹L. Yan, J. F. Li, C. Suchicital, and D. Viehland, *Appl. Phys. Lett.* **89**, 132913 (2006).